International Journal of
INTELLIGENT SYSTEMS AND APPLICATIONS IN ENGINEERING
ISSN:2147-6799 www.ijisae.org Original Research Paper

Analysis of Viscous Shear Effect in the Boundary Layer Region of Porous Medium of Infinitely Long Journal Bearing

M. Somashekhar[1a,2], G. K. Kalavathi[2, b*], M. G. Vasundhara[3,c], P. A. Dinesh[4,d], and E. L. Pradeesh[5,e]

Submitted: 11/09/2023 **Revised:** 23/10/2023 **Accepted:** 02/11/2023

Abstract. This study analyses the effect of viscous shear over a permeable boundary. A viscous shear term called structural parameter is considered to derive a generalized Reynolds equation that governs the lubricant flow. The performance of structural parameters is then analyzed using infinitely long journal-bearing approximation. Reynolds boundary condition is considered in long bearing approximation. It is found that structural parameter adversely affects the load carrying capacity (LCC) and decreases friction, however attitude angle is not affected significantly. Also, the analysis indicates that the effect of viscous shear force is prominent when the bearing operates at a lower eccentric ratio and lower permeability. It is then used to analyse the narrow bearing approximation. Analysis shows that the combination of the structural parameter, permeability parameter and eccentricity ratio will significantly increase the effect of the boundary layer region within the porous region, this boosts load-carrying capacity and reduces friction.

Key Words: *viscous shear term, heterogeneous slip/no-slip surface, roughness. Structural Parameter.*

Introduction: In industries, porous journal bearings have been widely used for a long time because these bearings do not need exterior oil once the oil is impregnated in porous material. The porous material injects oil and forms a hydrodynamic oil film when the journal bearing takes speed. Morgan and Cameron [1] are original authors who have studied the hydrodynamic theory of porous journal bearings. P R K Murthi [2–4] studied the hydrodynamic lubrication of metal bearings. J R Linn and C C Hwang [5-6] studied the viscous shear effect over a permeable region of porous journal bearing. Tyrone Dass et.al [7] examined the combined effect of velocity slip, variable viscosity and the couple stress lubricant on a finite journal bearing. Kumar M et.al [8] investigate how the hydrodynamic journal bearing performance is affected by the transverse and longitudinal sinusoidal, full, and half-wave texture roughness pattern. Zhu S [9] analyses the Thermohydrodynamic lubrication of journal bearing considering surface roughness and couple stress. Additionally, the finite difference numerical method is used to get the performance parameters under the influence of journal misalignment, surface roughness, couple stress, and temperature impact. Tian Z et.al [10] Talking about the study, which concentrated on the dynamic characteristics of long journal bearings, it aimed to show how surface roughness affects the dynamic performances of long bearings. The improved Reynolds equation was established using the long-bearing assumptions and the Christensen stochastic model. The numerical integration method was utilized to determine the updated Reynolds equation. K Gururajan and J Prakash [11–14] effect of roughness and arbitrary wall thickness of

1 Department of Mathematics, Rajeev Institute of Technology, Hassan, Visvesvaraya Technological University, Belagavi, Karnataka, India
2 Department of Mathematics, Malnad College of Engineering, Hassan, Visvesvaraya Technological University, Belagavi, Karnataka, India
3 Department of Mechanical Engineering, Malnad College of Engineering, Hassan, Visvesvaraya Technological University, Belagavi, Karnataka, India
4 Department of Mathematics, Ramaiah Institute of Technology, Bangalore,
Visvesvaraya Technological University, Belagavi, Karnataka, India
5 Department of Mechatronics, Bannari Amman Institute of Technology, Sathyamangal, Tamilnadu.
asomashekharmaths@rediffmail.com, bgkk@mcehassan.ac.in, cmgv@mcehassan.ac.in, ddineshdpa@msrit.edu, epradeesh.dmt@gmail.com.

porous journal bearing. Salant and Fortier [15-16] studied the heterogeneous slip/No-slip surface. Kalavathi et.al [17–22] studied the effect of roughness and magnetic field by considering the heterogeneous slip/No-slip surface.

The performance of porous journal bearings has been evaluated by S. Sharma et al. [23] using spherically generated textures, taking into account the textures' placement at various eccentricity ratios. B A Abbas et al. [24] investigate the journal bearing performance by taking into account the combined effects of cavitation, bearing liner elasticity, and the nonlinearity behaviour of the working fluid. The study conducted by Nur Cahyo and colleagues [25] explores the impact of engineered surface roughness on the performance of bearings lubricated with Bingham plastic. They utilized a three-dimensional computational fluid dynamics (CFD) model of a journal bearing for their investigation, which also took cavitation into account. Dhanishta Sirohi along with colleagues [26] researched the fact that a pocket is more advantageous than a pad with bumps or grooves for increasing the minimum film thickness and lowering the coefficient of friction. Rolling Contact Fatigue (RCF) was evaluated by Shuhei Kajiwara and colleagues [27] revealing issues such as wear, flaking, and crack propagation. To thoroughly examine the effect of cycle count on surface roughness, the RCF test was carried out in water with a thrust stress of 2,300 N. Hwang et al. [28] have studied the unique characteristics of electrohydrodynamic rotational lubrication analysis in journal-bearing systems. To simulate electrohydrodynamic lubrication, they created a virtual environment by integrating Elasto-Hydro-Dynamic (EHD) and Multi-Body Dynamic (MBD) solvers, incorporating lubricant into the model.

In this study, the viscous shear term is included in the Navier-Stokes equation and Brinkmann-extended Darcy equation to derive a modified Reynolds equation. This investigates the effects of viscous shear force in a porous medium called a structural parameter on bearing characteristics. This viscous shear force penetrates the permeable region to form an effective boundary layer. The generalized Reynolds equation is derived by considering Navier slip boundary conditions for heterogeneous slip/No-slip surfaces. Then the analysis is given for the hydrodynamic infinitely long journal bearing by considering the Reynolds boundary condition.

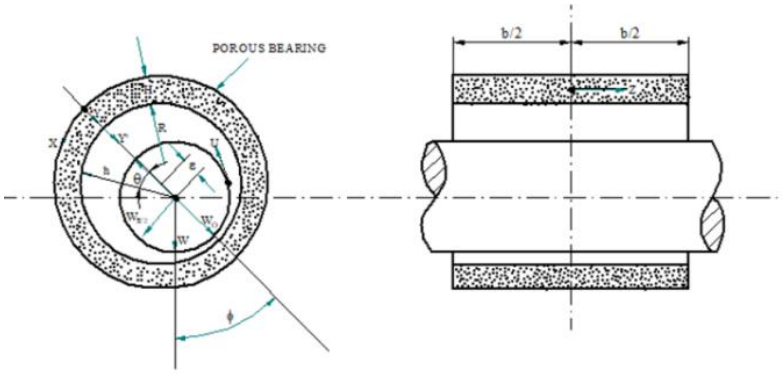

Fig. 1a. *Porous Journal Bearing.*

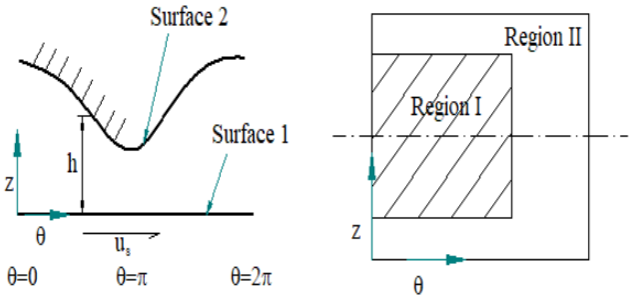

Fig. 1b. *Slip/No-Slip BC*

2. Analysis

The physical configuration of the porous journal bearing and the bearing surface with heterogeneous slip/No-slip surface are shown in Figure 1(a) and Figure 1(b). The porous bearing is press-fitted in a housing and fluid film supports non-porous journal bearing. Some of the assumptions are made while deriving Reynolds equations namely Laminar flow of fluid is considered, the fluid flow in steady state condition, on oil film external force is not acting and across the fluid film, there is no variations of pressure.

The reduced Brinkman-extended Darcy equation [29] is given by

$$\bar{\mu}\frac{\partial^2 \bar{u}}{\partial y^2} - \frac{\mu}{\mathrm{K}}\bar{u} = \frac{\partial p}{\partial x}. \tag{1}$$

$$\bar{\mu}\frac{\partial^2 \bar{w}}{\partial y^2} - \frac{\mu}{\mathrm{K}}\bar{w} = \frac{\partial p}{\partial z}. \tag{2}$$

$$\frac{\partial p}{\partial y} = 0. \tag{3}$$

Solving equation (1) by dividing $\bar{\mu}$.

The continuity equation in the porous medium is given by

$$\frac{\partial q_x}{\partial x} + \frac{\partial q_y}{\partial y} + \frac{\partial q_z}{\partial z} = 0. \tag{4}$$

Journal and bearing are assumed to be designed in such a way that bearing film thickness assumes

$$h = C(1 + \epsilon\, cos\theta) + h_s. \tag{5}$$

Navier boundary condition is modelled by considering slip, since in region-1 slip velocity is directly proportional to surface shear stress [12]

At y = 0; $\bar{u} = u_s$, $\bar{v} = -V_0$, $\bar{w} = 0$. (6)

At $y = h$; $\bar{u} = -\alpha\mu\frac{\partial u}{\partial y}$, $\bar{v} = 0$, $\bar{w} = -\alpha\mu\frac{\partial w}{\partial y}$. (7)

Solving second order differential equation (1) and (2) respectively, we have

$$\bar{u} = C_1 cosh\left[\left(\frac{\mu}{\bar{\mu}}\right)^{\frac{1}{2}}\frac{1}{K^{\frac{1}{2}}}y\right] + C_2 sinh\left[\left(\frac{\mu}{\bar{\mu}}\right)^{\frac{1}{2}}\frac{1}{K^{\frac{1}{2}}}y\right] - \frac{K}{\mu}\frac{\partial p}{\partial x}. \tag{8}$$

$$\bar{w} = C_3 \cosh\left[\left(\frac{\mu}{\bar{\mu}}\right)^{\frac{1}{2}}\frac{1}{K^{\frac{1}{2}}}y\right] + C_4 \sinh\left[\left(\frac{\mu}{\bar{\mu}}\right)^{\frac{1}{2}}\frac{1}{K^{\frac{1}{2}}}y\right] - \frac{K}{\mu}\frac{\partial p}{\partial z}. \tag{9}$$

Using boundary condition (6) and (7), we obtain the velocity components

$$\bar{u} = \left\{\left(cosh\left[\frac{y}{\beta \mathrm{K}^{\frac{1}{2}}}\right] - sinh\left[\frac{y}{\beta \mathrm{K}^{\frac{1}{2}}}\right]\right) + \left(\frac{cosh\left[\frac{h}{\beta \mathrm{K}^{\frac{1}{2}}}\right] + \frac{\alpha\mu}{\beta K^{\frac{1}{2}}} sinh\left[\frac{h}{\beta \mathrm{K}^{\frac{1}{2}}}\right]}{\sinh\left[\frac{h}{\beta \mathrm{K}^{\frac{1}{2}}}\right] + \frac{\alpha\mu}{\beta K^{\frac{1}{2}}} cosh\left[\frac{h}{\beta \mathrm{K}^{\frac{1}{2}}}\right]}\right)\right\} u_s + \frac{K}{\mu}\frac{\partial p}{\partial x}\left\{\left(cosh\left[\frac{y}{\beta \mathrm{K}^{\frac{1}{2}}}\right] + sinh\left[\frac{y}{\beta \mathrm{K}^{\frac{1}{2}}}\right]\right)\left(\frac{1 - cosh\left[\frac{h}{\beta \mathrm{K}^{\frac{1}{2}}}\right] - \frac{\alpha\mu}{\beta K^{\frac{1}{2}}} sinh\left[\frac{h}{\beta \mathrm{K}^{\frac{1}{2}}}\right]}{\sinh\left[\frac{h}{\beta \mathrm{K}^{\frac{1}{2}}}\right] + \frac{\alpha\mu}{\beta K^{\frac{1}{2}}} cosh\left[\frac{h}{\beta \mathrm{K}^{\frac{1}{2}}}\right]}\right) - 1\right\}. \tag{10}$$

$$\bar{w} = \frac{K}{\mu}\frac{\partial p}{\partial z}\left\{\left(cosh\left[\frac{y}{\beta \mathrm{K}^{\frac{1}{2}}}\right] + sinh\left[\frac{y}{\beta \mathrm{K}^{\frac{1}{2}}}\right]\right) + \left(\frac{1 - cosh\left[\frac{h}{\beta \mathrm{K}^{\frac{1}{2}}}\right] - \frac{\alpha\mu}{\beta K^{\frac{1}{2}}} sinh\left[\frac{h}{\beta \mathrm{K}^{\frac{1}{2}}}\right]}{\sinh\left[\frac{h}{\beta \mathrm{K}^{\frac{1}{2}}}\right] + \frac{\alpha\mu}{\beta K^{\frac{1}{2}}} cosh\left[\frac{h}{\beta \mathrm{K}^{\frac{1}{2}}}\right]}\right) - 1\right\}. \tag{11}$$

where $\beta = \left(\frac{\bar{\mu}}{\mu}\right)^{\frac{1}{2}}$

Integrating equation (10) and (11) & $\bar{v}$ with respect y we have

$$q_x = \int_0^h \bar{u}dy = u_s\beta K^{\frac{1}{2}}\left\{\frac{cos\left[\frac{h}{\beta K^{\frac{1}{2}}}\right]+\frac{\alpha\mu}{\beta K^{\frac{1}{2}}}sin\left[\frac{h}{\beta K^{\frac{1}{2}}}\right]-1}{sin\left[\frac{h}{\beta K^{\frac{1}{2}}}\right]+\frac{\alpha\mu}{\beta K^{\frac{1}{2}}}cos\left[\frac{h}{\beta K^{\frac{1}{2}}}\right]}\right\} + \frac{K}{\mu}\frac{\partial p}{\partial x}\beta K^{\frac{1}{2}}\left\{\frac{\left(\frac{\alpha\mu}{\beta K^{\frac{1}{2}}}-\frac{h}{\beta K^{\frac{1}{2}}}\right)sin\left[\frac{h}{\beta K^{\frac{1}{2}}}\right]+\left(2-\frac{h}{\beta K^{\frac{1}{2}}}\times\frac{\alpha\mu}{\beta K^{\frac{1}{2}}}\right)cos\left[\frac{h}{\beta K^{\frac{1}{2}}}\right]-2}{sin\left[\frac{h}{\beta K^{\frac{1}{2}}}\right]+\frac{\alpha\mu}{\beta K^{\frac{1}{2}}}cos\left[\frac{h}{\beta K^{\frac{1}{2}}}\right]}\right\}. \quad (12)$$

$$q_y = \int_0^h \bar{v}dy = (V_h - V_0). \quad (13)$$

$$q_z = \int_0^h \bar{w}dy = \frac{K}{\mu}\frac{\partial p}{\partial z}\beta K^{\frac{1}{2}}\left\{\frac{\left(\frac{\alpha\mu}{\beta K^{\frac{1}{2}}}-\frac{h}{\beta K^{\frac{1}{2}}}\right)sin\left[\frac{h}{\beta K^{\frac{1}{2}}}\right]+\left(2-\frac{h}{\beta K^{\frac{1}{2}}}\times\frac{\alpha\mu}{\beta K^{\frac{1}{2}}}\right)cos\left[\frac{h}{\beta K^{\frac{1}{2}}}\right]-2}{sin\left[\frac{h}{\beta K^{\frac{1}{2}}}\right]+\frac{\alpha\mu}{\beta K^{\frac{1}{2}}}cos\left[\frac{h}{\beta K^{\frac{1}{2}}}\right]}\right\}. \quad (14)$$

Substitute (12), (13) and (14) in continuity equation (4) we obtain the Reynolds equation in porous medium.

$$\frac{\partial}{\partial x}\left[M_2\frac{\partial p}{\partial x}\right] + \frac{\partial}{\partial z}\left[M_2\frac{\partial p}{\partial z}\right] = -\frac{\mu}{K}u_s\frac{\partial}{\partial x}[M_1] - \frac{\mu}{K}\frac{1}{C}(V_h - V_0). \quad (15)$$

where

$$M_1 = \frac{\beta}{\sigma_0}\left\{\frac{cos\left[\frac{h}{\beta K^{\frac{1}{2}}}\right]+\frac{\alpha\mu}{\beta K^{\frac{1}{2}}}sin\left[\frac{h}{\beta K^{\frac{1}{2}}}\right]-1}{sin\left[\frac{h}{\beta K^{\frac{1}{2}}}\right]+\frac{\alpha\mu}{\beta K^{\frac{1}{2}}}cos\left[\frac{h}{\beta K^{\frac{1}{2}}}\right]}\right\}. \quad (16)$$

$$M_2 = \frac{\beta}{\sigma_0}\left\{\frac{\left(\frac{\alpha\mu}{\beta K^{\frac{1}{2}}}-\frac{h}{\beta K^{\frac{1}{2}}}\right)sin\left[\frac{h}{\beta K^{\frac{1}{2}}}\right]-2+\left(2-\frac{h}{\beta K^{\frac{1}{2}}}\times\frac{\alpha\mu}{\beta K^{\frac{1}{2}}}\right)cos\left[\frac{h}{\beta K^{\frac{1}{2}}}\right]}{sin\left[\frac{h}{\beta K^{\frac{1}{2}}}\right]+\frac{\alpha\mu}{\beta K^{\frac{1}{2}}}cos\left[\frac{h}{\beta K^{\frac{1}{2}}}\right]}\right\}. \quad (17)$$

The journal surface in x- direction is fixed and non-porous, V_h= 0 and in z-direction velocity component $V_0 = -\frac{K}{\mu}H_0\left[\frac{\partial^2 p}{\partial x^2}+\frac{\partial^2 p}{\partial z^2}\right]$ substituting V_h and V_0 in equation (15) & simplifying we get,

$$\frac{\partial}{\partial x}\left[\left(M_2 + \frac{KH_0}{C^3}\sigma_0^2\right)\frac{\partial p}{\partial x}\right] + \frac{\partial}{\partial z}\left[\left(M_2 + \frac{KH_0}{C^3}\sigma_0^2\right)\frac{\partial p}{\partial z}\right] = -\frac{\mu u_s}{K}\frac{\partial}{\partial x}[M_1]. \quad (18)$$

Using non-dimensional parameters:

$$A = \frac{\alpha\mu}{C}, \sigma_0 = \frac{C}{K^{\frac{1}{2}}}, \; H = \frac{h}{C}, \varphi = \frac{KH_0}{C^3}. \quad (19)$$

the dimensionless equation (18) is given by

$$\frac{\partial}{\partial x}\left[(M_2 + \sigma_0^2\varphi)\frac{\partial p}{\partial x}\right] + \frac{\partial}{\partial z}\left[(M_2 + \sigma_0^2\varphi)\frac{\partial p}{\partial z}\right] = -\frac{\mu u_s}{K}\frac{\partial}{\partial x}[M_1]. \quad (20)$$

Using Christensen's stochastic theory [30], the modified Reynolds equation becomes

$$\frac{\partial}{\partial x}\left[E\{M_2^* + \sigma_0^2\varphi\}\frac{\partial p}{\partial x}\right] + \frac{\partial}{\partial z}\left[E\{M_2^* + \sigma_0^2\varphi\}\frac{\partial p}{\partial z}\right] = -\frac{\mu u_s}{K}E\left\{\frac{\partial}{\partial x}[M_1^*]\right\}. \quad (21)$$

where

$$M_1^* = \frac{\beta}{\sigma_0}\left[\frac{cosh\left(\frac{H\sigma_0}{\beta}\right)+\frac{A\sigma_0}{\beta}sinh\left(\frac{H\sigma_0}{\beta}\right)-1}{sinh\left(\frac{H\sigma_0}{\beta}\right)+\frac{A\sigma_0}{\beta}cosh\left(\frac{H\sigma_0}{\beta}\right)}\right]. \quad (22)$$

$$M_2^* = \frac{\frac{\beta}{\sigma_0}\left[\left(\frac{A\sigma_0}{\beta}-\frac{H\sigma_0}{\beta}\right)sinh\left(\frac{H\sigma_0}{\beta}\right)-2+\left(2-\frac{H\sigma_0}{\beta}\times\frac{A\sigma_0}{\beta}\right)cosh\left(\frac{H\sigma_0}{\beta}\right)\right]}{sinh\left(\frac{H\sigma_0}{\beta}\right)+\frac{A\sigma_0}{\beta}cosh\left(\frac{H\sigma_0}{\beta}\right)}. \quad (23)$$

According to Christensen, roughness is classified as Longitudinal roughness & Transverse roughness pattern.

Longitudinal roughness is given by

$$\frac{\partial}{\partial x}\left[E\{M_2^* + \sigma_0^2\varphi\}\frac{\partial\{E(p)\}}{\partial x}\right] + \frac{\partial}{\partial z}\left[\left\{\frac{1}{E\left(1/M_2^*\right)} + \sigma_0^2\varphi\right\}\frac{\partial\{E(p)\}}{\partial z}\right] = -\frac{\mu u_s}{K}\frac{\partial}{\partial x}[E\{M_1^*\}]. \quad (24)$$

Transverse roughness is given by

$$\frac{\partial}{\partial x}\left[\left\{\frac{1}{E\left(1/M_2^*\right)} + \sigma_0^2\varphi\right\}\frac{\partial\{E(p)\}}{\partial x}\right] + \frac{\partial}{\partial z}\left[E\{M_2^* + \sigma_0^2\varphi\}\frac{\partial\{E(p)\}}{\partial z}\right] = -\frac{\mu u_s}{K}\frac{\partial}{\partial x}\left[\frac{E\left\{M_1^*/M_2^*\right\}}{E\left\{1/M_2^*\right\}}\right]. \quad (25)$$

By journal-bearing theory neglecting $\frac{\partial}{\partial z}E(p)$ in equation (24) we have

$$\frac{\partial}{\partial x}\left[E\{M_2^* + \sigma_0^2\varphi\}\frac{\partial\{E(p)\}}{\partial x}\right] = -\frac{\mu u_s}{K}\frac{\partial}{\partial x}[E\{M_1^*\}]. \quad (26)$$

or

$$\frac{d}{d\theta}\left[\{E(M_2^*) + \sigma_0^2\varphi\}\frac{\partial}{\partial\theta}\{E(p)\}\right] = -\frac{\mu u_s}{K}\,R\frac{d}{d\theta}\{E(M_1^*)\}. \quad (27)$$

here, $x = R\theta$

For the lubricant in the film region, the Reynolds boundary conditions are given by

$$E(p) = 0 \quad @\ \theta = 0. \quad (28)$$

$$\frac{d}{d\theta}E(p) = 0 \quad @\ \theta = \theta_2. \quad (29)$$

$$E(p) = 0 \quad @\ \theta = \theta_2. \quad (30)$$

3. Mean pressure

By Integrating equation (27) twice w.r.t to θ and using boundary conditions (28) and (29) we get

$$E(p) = -\frac{\mu u_s R}{K}\int_0^\theta \frac{\{E(M_1^*)\} - [E(M_1^*)]_{\theta=\theta_2}}{\{E(M_2^*)+\sigma_0^2\varphi\}}\,d\theta. \quad (31)$$

Non-dimensionalizing,

$$\bar{p} = -\int_0^\theta \frac{\{E(M_1^*)\} - [E(M_1^*)]_{\theta=\theta_2}}{\{E(M_2^*)+\sigma_0^2\varphi\}}\,d\theta. \quad (32)$$

The cavitation angle is calculated by using the condition

$$\bar{p}(\theta_2) = 0. \quad (33)$$

This gives

$$\int_0^{\theta_2}\frac{\{E(M_1^*)\}}{\{E(M_2^*)+\sigma_0^2\varphi\}}\,d\theta - [E(M_1^*)]_{\theta=\theta_2}\int_0^{\theta_2}\frac{d\theta}{\{E(M_2^*)+\sigma_0^2\varphi\}} = 0. \quad (34)$$

It is difficult to solve equation (34) analytically. Hence the angle θ_2 is evaluated numerically using the bisection method.

4. Bearing characteristics

Characteristics of the bearing are determined using equation (32) by depicting film pressure distribution. Hence, it is customary to assume over $0 \le \theta \le \theta_2$ of bearing arc, the oil film extends and ignores the negative pressure region $\theta_2 < \theta < 2\pi$.

5. Mean load capacity

Integrating equation (32) in the circumferential direction between the limit $\theta = 0$ to $\theta = \theta_2$ and by neglecting the negative region, the load capacity across the line of center, w_0 is obtained as

$$W_0 = -\int_0^{\theta_2} \bar{p}\, cos\theta\, d\theta. \quad (35)$$

The load capacity across the line of center, $w_{\frac{\pi}{2}}$ is obtained as

$$W_{\frac{\pi}{2}} = \int_0^{\theta_2} \bar{p}\, sin\theta\, d\theta. \quad (36)$$

6. Mean friction force

On the journal bearing, shear stress τ_s given by

$$\tau_s = \frac{\mu u_s}{K^{\frac{1}{2}}}\left[\frac{-1}{\beta\left\{\sinh\left(\frac{H\sigma_0}{\beta}\right)+\frac{A\sigma_0}{\beta}cosh\left(\frac{H\sigma_0}{\beta}\right)\right\}}\right] + K^{\frac{1}{2}}\frac{\partial p}{\partial x}\left[\frac{cosh\left(\frac{H\sigma_0}{\beta}\right)-1}{\beta\left\{\sinh\left(\frac{H\sigma_0}{\beta}\right)+\frac{A\sigma_0}{\beta}cosh\left(\frac{H\sigma_0}{\beta}\right)\right\}}\right]. \quad (37)$$

$$E(\tau_s) = K^{\frac{1}{2}}\frac{\partial}{\partial x}[E(P)]E\left[\frac{cosh\left(\frac{H\sigma_0}{\beta}\right)-1}{\beta\left\{\sinh\left(\frac{H\sigma_0}{\beta}\right)+\frac{A\sigma_0}{\beta}cosh\left(\frac{H\sigma_0}{\beta}\right)\right\}}\right] - \frac{\mu u_s}{K^{\frac{1}{2}}}E\left[\frac{1}{\beta\left\{\sinh\left(\frac{H\sigma_0}{\beta}\right)+\frac{A\sigma_0}{\beta}cosh\left(\frac{H\sigma_0}{\beta}\right)\right\}}\right]. \quad (38)$$

Mean friction force acting on journal surfaces is

$$E(F) = \frac{\sigma_0}{\beta}\left\{\int_0^{\theta_2}\left\{\frac{d\bar{p}}{d\theta}E[F(H,\sigma_0,A,\beta)] - E[G(H,\sigma_0,A,\beta)]\right\}d\theta - \int_{\theta_2}^{2\pi}\left[\frac{H(\theta_2)}{H}E[G(H,\sigma_0,A,\beta)]d\theta\right]\right\}. \quad (39)$$

where $\frac{d\bar{p}}{d\theta} = \left[\frac{\left\{E(M_1^*)-E\left((M_1^*)_{\theta=\theta_2}\right)\right\}}{\{E(M_2^*)+\sigma_0\phi\}}\right]$.

7. Result and discussion

The concept enhances understanding of fluid film behaviour under load, supporting the development of lubrication theories. Engineers use this to assess lubricant flow, load capacity, and friction before adjusting for finite-length effects. To evaluate the bearing characteristics the values of the parameter as listed as follows

Eccentricity, $\varepsilon = 0.1, 0.2, 0.3, 0.4, 0.5, 0.6, 0.7, 0.8$

Permeability parameter, $\phi = 0.00001, 0.0001, 0.001, 0.01, 0.1, 1$

Structural parameter, $\beta = 0.1, 0.2, 0.3, 0.4, 0.5$ [5]

Roughness parameter, $C = 0.1, 0.2, 0.3, \ldots\ldots, 0.8$

Slip parameter, $A = 0, 5, 10, 15, 20$

The structural parameter (β) depends on the permeability of the porous medium, β is set to equal to zero implies within the porous media effective viscosity $\bar{\mu}$ is neglected hence Brinkman's [5] equation (1) and (2) reduces to the Darcy equation. In the lubricant film, a boundary layer region is formed since viscous shear penetrates the porous medium due to this pressure inside the bearing increases. Hence the load-carrying capacity increases and friction decreases. In this model, the non-dimensional parameter $\sigma_0 = {C}/{K^{\frac{1}{2}}}$ takes the values 0.1 and 0.2.

Bearing characteristics depend on the non-dimensional parameters like structural parameter β, Eccentricity ε, Permeability parameter ψ, Roughness parameter C and Slip parameter A. It is interesting to note that as structural parameter $\beta \to 0$, the Reynolds equation obtained is identical to that derived by Kalavathi et.al [7]. It is also noted that structural parameter $\beta \to 0$ and slip parameter $A \to 0$ the expression so obtained is identical to the case study Gururajan and Prakash [8]. The definite integrals in various expressions are evaluated using the Gaussian16 point quadrature formula, as it gives the correctness up to four decimal places. The cavitation (θ_2) is found by using the Bisection method.

8. Angular extent of the oil film

The angular extent of the oil film (θ_2) for different values of eccentricity ratio is shown in Fig. 2 for different values of β, for the fixed values of $\psi = 0.1$, $C = 0.2$ and Slip parameter $A = 5$. Says that the maximum roughness pattern is 20% diameter clearance of the bearing. Fig. 3 is plotted cavitation angle θ_2 versus permeability ψ for different Structural parameters β. In all these graphs it is observed that as structural parameter increases θ_2 decreases. Fig. 4 is plotted cavitation angle θ_2 versus eccentricity for different Roughness parameter C. It is noted that θ_2 decrease with increasing roughness parameter.

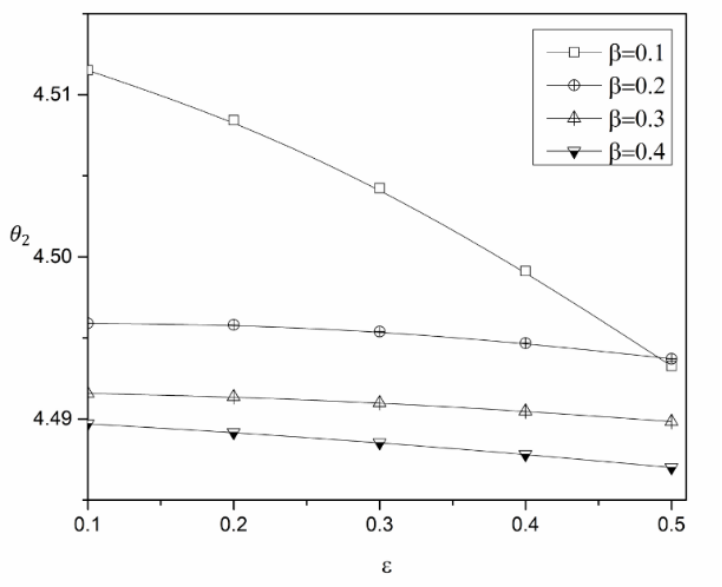

Fig. 2: θ_2 verses Eccentricity ε for different Structural parameters β with $\psi = 0.1$ and $C = 0.2$.

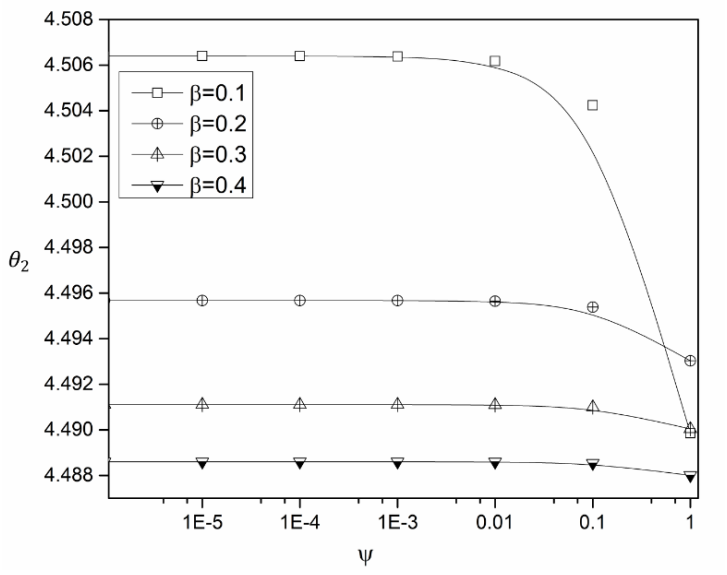

Fig. 3: θ_2 verses ψ for different Structural parameters β with $\varepsilon = 0.3$ and $C = 0.2$

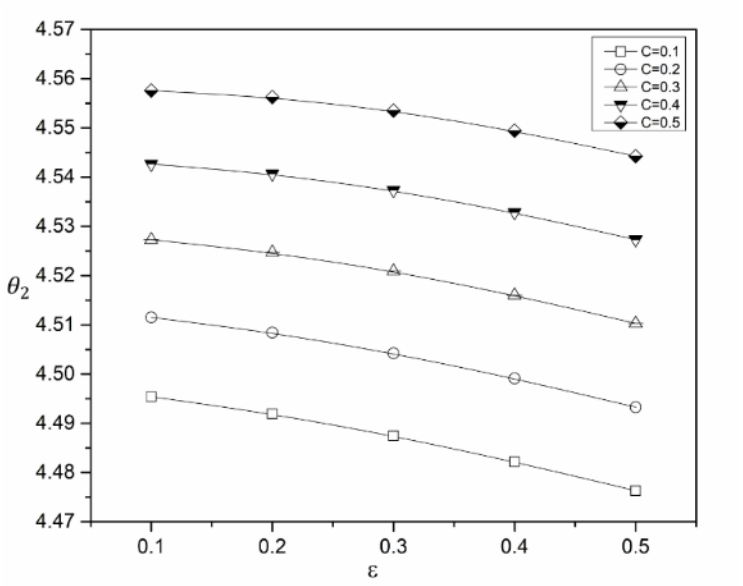

Fig. 4: θ_2 verses ε for various Roughness parameters C with $\psi = 0.1$ and $\beta = 0.1$.

9. Load carrying capacity (LCC)

Variation of mean LCC is shown in Fig. 5 to Fig. 8. When the bearing runs at eccentricity ratios approaching the hydrodynamic limit, substantial deviations are observed. An increase in LCC is found for higher values of A shown in Figure 5. The roughness pattern will not affect the LCC shown in Fig. 6. LCC decreases with increasing values of β but increases with increasing ε shown in Fig. 6, Fig. 7 and Fig. 8 shows LCC verses ψ for fixed ε, A and C. It is found that LCC decreases with increasing ψ and lower values of β.

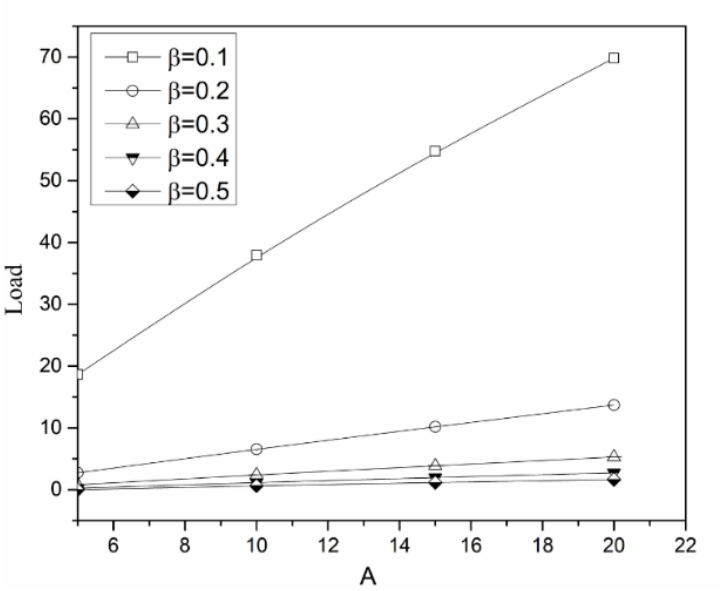

Fig. 5: *Load versus A for Different values of Structural parameter β with $\varepsilon = 0.5$, $\psi = 0.1$ and $C = 0.3$.*

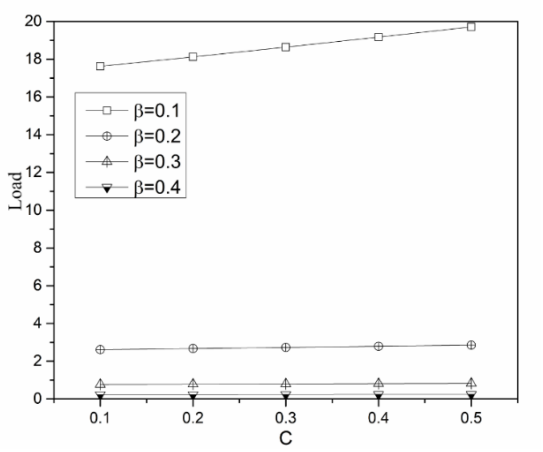

Fig. 6: Load variation of load with C for various Structural parameter β with $\varepsilon = 0.5$, $\psi = 0.1$ and $A = 5$.

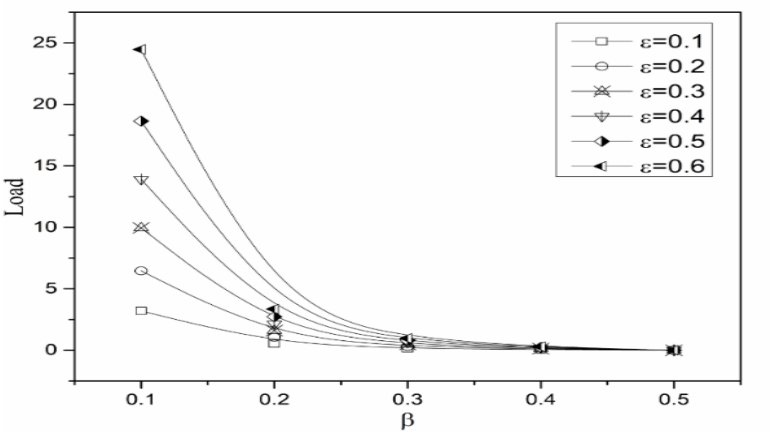

Fig. 7: Load versus Structural parameter β for various ε with $\psi = 0.1$, $A = 5$ and $C = 0.3$

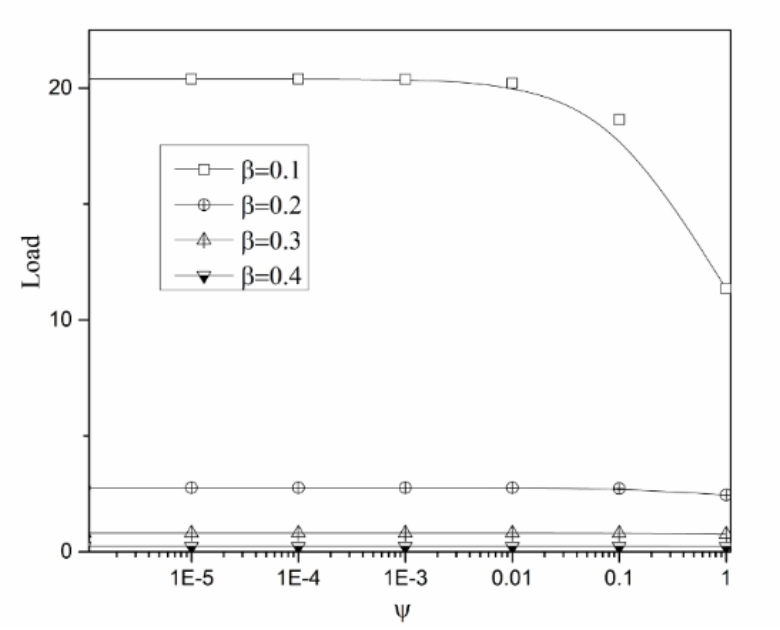

Fig. 8: Load versus ψ for various Structural parameters β with $\varepsilon = 0.5$, $A = 5$ and $C = 0.3$

10. Friction

Variations of frictional forces are presented in Fig. 9 to Fig. 11. Fig. 9 shows Friction increases with increasing values of C and decreases for lesser values of β decreases. No variation of friction is observed for variations of ψ and friction decreases with a lesser value of β as shown in Fig. 10. Fig. 11 shows friction increases with an increase in β.

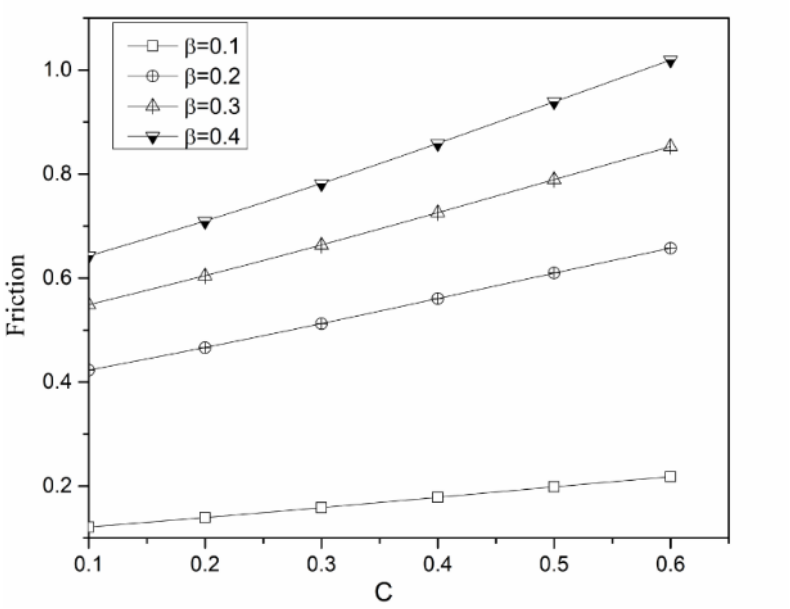

Fig. 9: Variation of friction with C for different β with $\varepsilon = 0.1$ and $\psi = 0.1$

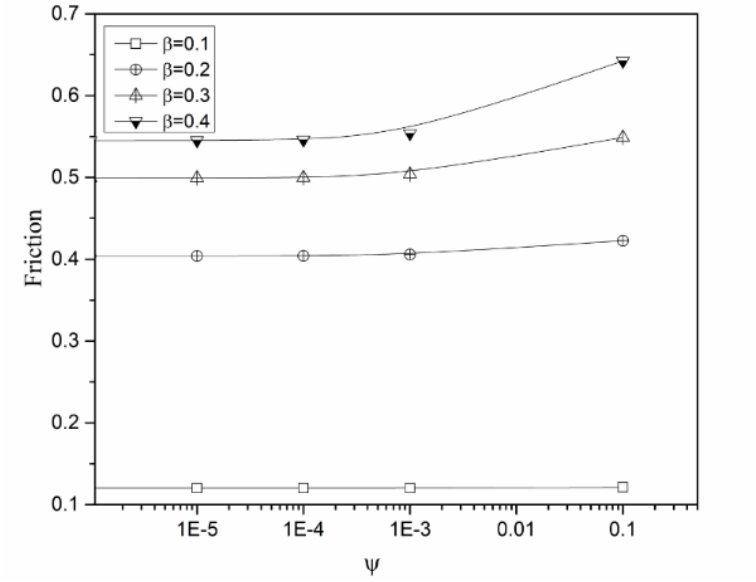

Fig. 10: *Friction versus ψ for different β with $\varepsilon = 0.8$ and $C = 0.1$*

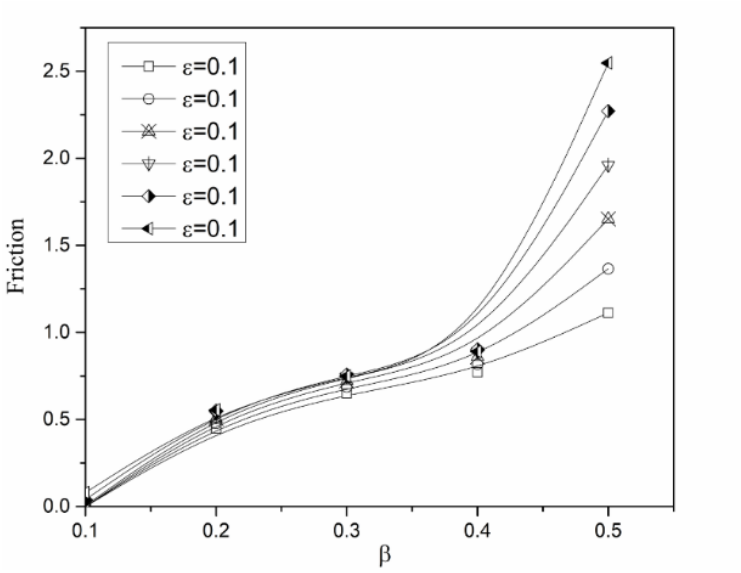

Fig.11: *Friction versus Structural parameter* β *for various values eccentricity ratio* ε *with* $\psi = 0.1$ *and* $C = 0.1$

11. Attitude angle

The focus of the journal center for different values of ψ is shown in Table 1 with fixed $C = 0.2$, $A = 5$ And $\varepsilon = 0.3$. It is observed that the effect of viscous shear is not very significant for most of the operating parameters.

Table 1:

ε	$\psi = 1$	$\psi = 0.01$	$\psi = 0$
0.1	75.27468	75.65541	75.65971
0.2	77.62191	78.46446	78.47405
0.3	80.16419	81.53897	81.55467
0.4	82.8749	84.83667	84.85911
0.5	85.7209	88.304	88.33355

12. JUSTIFICATION

It is observed from Fig. 12 that cavity angle θ_2 for $A \longrightarrow 0$, $\beta \longrightarrow 0$ and $\sigma = 0.1$, $C = 0.2$, $\psi = 0.1$ is at most the same as the case studied by K Gururajan and J Prakash [11].

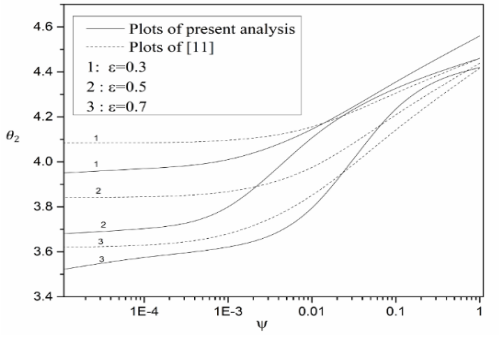

Fig. 12: Cavitation angle θ_2 ***verses Permeability parameter*** ψ ***for different values eccentricity.***

13. Conclusion

A complete characteristics analysis of infinitely long journal bearing by considering heterogeneous surfaces are analyzed. Christensen's stochastic model is used to study the effect of roughness. To analyze the hydrodynamic lubrication of long porous journal bearing, Brinkman's extended Darcy model is used. The viscous shear term is made active in the porous region, due to the presence of the viscous shear term a boundary layer region is formed.

(i) Presence of Structural parameter β, a significant increase in LCC is found as also found the reduction of friction.

(ii) The combination of structural parameters β, ϕ and ε respectively significantly increases the effect of boundary layer region within porous region. This results in good characteristics of infinitely long journal bearing.

Nomenclature

b	Breadth of bearing	$\bar{w}$	z-component of velocity in the porous medium
C	Radial clearance	W	Total load capacity of the bearing
d	Diameter of journal	w_0	Maximum allowable load per unit length of central
e	Eccentricity	W_0^*	$\frac{w_0}{\mu u_s b}\frac{C^2}{r^2}$ (non-dimensional)
f	Coefficient of friction	$w_{\frac{\pi}{2}}$	Maximum load acting in a direction perpendicular to the center line
F_j^*	$\frac{F_j C}{\mu u_s b r}$ (non-dimensional)	$w_{\frac{\pi}{2}}^*$	$\frac{w_{\frac{\pi}{2}}}{\mu u_s b}\frac{C^2}{r^2}$ (non-dimensional)
h	Film thickness	**Greek Symbol**	
h_s	Roughness parameter	ε	Eccentricity ratio, e/C (non-dimensional)
H	h/C (non-dimensional)	$\Delta\frac{d^2}{b^2}$	Ocvrik number (non-dimensional)
K	Permeability of bearing material	β	Structural parameter, $\left(\frac{\mu}{\bar{\mu}}\right)^{\frac{1}{2}}$ (non-dimensional)
p	Pressure in the oil film	λ	b/2r, (non-dimensional)
p^*	$\frac{E(p)C^2}{\mu r u_s}$ (non-dimensional)	μ	Oil viscosity
r, θ, z	Cylindrical coordinates	$\bar{\mu}$	Effective viscosity
R	Radius of the journal	σ	$H/K^{1/2}$ (non-dimensional)
r_1	Inner radius of porous bearing	σ_0	$C/K^{1/2}$ (non-dimensional)
$\bar{u}$	x-component of velocity in the porous material	τ_s	Shearing stress on the journal
u_s	Surface velocity of the journal	Φ	Permeability parameter, Kr/C^3 (non-dimensional)
$\bar{v}$	y-component of velocity in the porous material	ψ	Attitude angle

Acknowledgement

Authors thankful for Department of Mathematics Malnad college of Engineering Hassan for support.

REFERENCES

[1] V. T. Morgan, A. Cameron. Mechanism of lubrication in porous metal bearings. Proc Conf on lubrication and Wear, Inst Mech Eng. 89 (1957) 151–157.

[2] P. R. K. Murti. Hydrodynamic lubrication of long porous bearings. Wear. 18 (1971) 449–460

[3] P. R. K. Murti. Hydrodynamic lubrication of finite porous bearings. Wear. 19 (1972) 113–115.

[4] P. R. K. Murti. Hydrodynamic lubrication of short porous bearings. Wear. 19 (1972) 17–25.

[5] J. R. Lin, C. C. Hwang. Lubrication of short porous journal bearings — use of the Brinkman-extended Darcy model. Wear. 161 (1993) 93–104.

[6] J. R. Lin, C. C. Hwang. Static and dynamic characteristics of long porous journal bearings: use of the Brinkman-extended Darcy model. J Phys D Appl Phys. 27 (1994) 634–643.

[7] T. Dass, S. R. Gunakala, D. M. G. Comissiong. The combined effect of couple stresses, variable viscosity and velocity-slip on the lubrication of finite journal bearings. Ain Shams Engineering Journal. 11(2020) 501–518.

[8] M. Kumar, K. N. Pandey. Enhancing journal bearing performance through surface texturing: A comprehensive review of latest developments and future prospects. Proceedings of the Institution of Mechanical Engineers, Part E: Journal of Process Mechanical Engineering. (2023) https://doi.org/10.1177/09544089231211230

[9] S. Zhu, X. Zhang. Thermohydrodynamic lubrication analysis of misaligned journal bearing considering surface roughness and couple stress. Proceedings of the Institution of Mechanical Engineers, Part J: Journal of Engineering Tribology. 236 (2022) 2243–2260.

[10] Z Tian, G. Chen. Discussion on dynamic characteristics of long journal bearings considering surface roughness. Advances in Mechanical Engineering. 14 (2022) :168781322211364.

[11] K. Gururajan and J. Prakash. Surface roughness effects in infinitely long porous journal bearings. Tribology Transactions. 121 (1999) 139–147.

[12] K. Gururajan, J. Prakash. Effect of Surface Roughness in a Narrow Porous Journal Bearing. J Tribol.122 (1999) 472–475.

[13] K. Gururajan, J. Prakash. Roughness effects in a narrow porous journal bearing with arbitrary porous wall thickness. Int J Mech Sci. 44 (2002) 1003–1016.

[14] K. Gururajan, J. Prakash. Effect of velocity slip in a narrow rough porous journal bearing". In proceedings of institution of mechanical Engineers. Part J: J Eng. Tribol. 217 (2003) 59–70. http://dx.doi.org/101243/135065003321164802

[15] R.F. Salant. Numerical Simulation of a Mechanical Seal with an Engineered Slip/No-Slip Face Surface. 17th Int. Conf. on Fluid Sealing, BHRG, Cranfield, UK. (2003) 15-28.

[16] R. F. Salant, A. E. Fortier. Numerical Analysis of a Slider Bearing with a Heterogeneous Slip/No-Slip Surface. Tribology Transactions. 47 (2004) 328–334.

[17] G. K. Kalavathi, K. Gururajan, P. A. Dinesh, G. Gurubasavaraj. Effect of surface roughness in a Narrow porous journal bearing with a heterogeneous slip/no-slip surface. International journal of Scientific and Innovative Mathematical Research. 12 (2014) 944–959.

[18] G. K. Kalavathi, P. A Dinesh, K. Gururajan. Numerical study of effect of roughness on porous long journal bearing with heterogeneous surface. Journal of the Nigerian Mathematical Society. 35 (2016) 468–487.

[19] G. K. Kalavathi, P. A. Dinesh, K. Gururajan. Influence of roughness on porous finite journal bearing with heterogeneous slip/no-slip surface. Tribol Int. 102(2016) 174–181.

[20] G. K. Kalavathi, F. A. Najar, M. G. Vasundhara. Performance characteristics of journal bearings (porous type): A coupled solution using Hartmann number and roughness parameter. 234 (2019) 668–675. https://doi.org/101177/1350650119886709

[21] G. K. Kalavathi, M. Somashekhar, M. G. Vasundhara, K. K. Yogesha. Analytical Study of Roughness on Tilted Pad Thrust Slider Bearing Improved by the Boundary Slippage. Applied Mechanics and Materials. 895 (2019) 70–75.

[22] G. K. Kalavathi, B. K. Yuvaraja, P. A. Dinesh, M. G. Vasundhara. Theoretical Study of influence of MHD in an infinitely long rough Porous Journal Bearing. IOP Conf Ser Mater Sci Eng (2021) 1189:012030.

[23] N. Sharma, S. Kango. Influence of High Permeability Parameter on the Performance of Textured Porous Journal Bearings. Tribology in Industry. 42 (2020) 370-381.

[24] B.A. Abass and M.A. Mahdi. Effect of Cavitation on the Performance of Journal Bearings Lubricated with Non-Newtonian Lubricant. Tribology in Industry. 42 (2020) 666-678.

[25] Nur Cahyo, P. Paryanto, Ariyana Dwiputra Nugraha, Arionmaro Simaremare, Indra Ardhanayudha Aditya, Bara Songka Laktona Siregar, Mohammad Tauviqirrahman. Effect of Engineered Roughness on the Performance of Journal Bearings Lubricated by Bingham Plastic Fluid Using Computational Fluid Dynamics (CFD). Lubricants 10 (2022) 333.

[26] Dhanishta Sirohi, Shipra Aggarwal. Numerical and Experimental Studies on Performance Enhancement of Thrust Pad Bearing Employing Surface Texture: A Review. Tribology in Industry. 45 (2023) 542-560.

[27] Shuhei Kajiwara, Takahiro Matsueda, Koshiro Mizobe, Katsuyuki Kida. Effect of Number of Cycles on Surface Roughness of PPS Thrust Bearings Under Rolling Contact Fatigue in Water. Materials Science forum, Scientific.net, Trans Tech Publication Ltd. Swizerland. 1101 (2023) 35-39.

[28] Hwang, Yunn-Lin, Adhitya. Electrohydrodynamic Rotational Lubrication Analysis on the Multi-Body Dynamic Properties of Journal-Bearing Systems. Defect and diffusion forum, Scientific.net, Trans Tech Publication Ltd. Swizerland.430 (2024) 33-39.

[29] M. H. Hamdan, R. M. Barron. Analysis of the Darcy-Lapwood and the Darcy-Lapwood-Brinkman models: significance of the laplacian. Appl Math Comput. 44 (1991) 121–141.

[30] H. CHRISTENSEN. Stochastic Models for Hydrodynamic Lubrication of Rough Surfaces. 18 (1969) 1013–1026.

http://dx.doi.org/101243/PIME_PROC_1969_184_074_02 18:1013–1026